12

A Scientific Approach to UHF RFID Systems Characterization

Ulrich Muehlmann
NXP Semiconductors
Austria

1. Introduction

RADIO Frequency Identification (RFID) technology gained a lot of attention in the last few years. Especially, RFID at ultra high frequencies (UHF) is very attractive for various applications in supply chain management or logistics (see Glidden & Schroeter, 2005). The long-range power transportation feature and the ultra low power consumption property of current transponder chips enable a remotely powered communication along several meters of distance in terms of energy transport and data exchange.

In supply chain management or other applications that rely on high volume throughput, passive transponders are used because this type of transponder can be attached and manufactured in high volume at extremely low cost in the range of a few $ cents (see Glidden et al., 2004). Furthermore, an advanced protocol layer (see ISO Standards, 2007) enables the inventory of hundreds of items per second (see Glidden et al., 2004 and Vogt, 2002) having a sophisticated anti-collision algorithm.

From the system perspective, a passive transponder must obtain its energy for operation out of the RF field generated by an interrogator. Aside from the market relevant aspects such as low system costs and high transparency of stock inventories, UHF seams to be an appropriate frequency range for long-range passive RFID systems because of the moderate path-loss of RF field propagation and acceptable insertion-loss of silicon (see Finkenzeller, 1999; De Vita & Iannaccone, 2005; Karthaus & Fischer, 2003). This is a conclusion coming out of several technical analyses. Known issues coming from classical radio communication apply to UHF RFID as well. The finite propagation velocity of electromagnetic waves causes compulsorily a superimposition of the radiated power commonly known as multi-path propagation with the consequence of signal fading and superimposed interference during communication (see Saunders, 1999). Without appropriate measures, UHF RFID systems will suffer from read performance degradation and unwanted interrogation in the surrounding area.

Applications in the supply chain management, like the inventory process during the flow of pallets carrying hundreds of items through multiple gates or dock-doors, must ensure high operational reliability because missing reads cause mismatch between in-stock databases and actual item count and would make the entire identification system unacceptable for RFID deployment. In order to ensure the operational reliability one has to identify all performance degradation factors causing interrogation errors. J. Mitsugi et al. have

Source: Development and Implementation of RFID Technology, Book edited by: Cristina TURCU,
ISBN 978-3-902613-54-7, pp. 554, February 2009, I-Tech, Vienna, Austria

published several studies dealing with readability degradation and field characterization related to UHF RFID applications (see Mitsugi & Hada, 2006; Mitsugi & Shibao, 2007; Mitsugi & Tokumasu, 2008). All these approaches are based on an extensive evaluation of the actual recorded field measurement data, illustrating the reading performance associated with a defined tag sensitivity threshold and with the maximum permitted interrogation power of the interrogator-to-tag forward link. Several theoretical and practical investigations (see Aroor & Deavours, 2007) have shown that the forward link limits the operational range and causes interrogation failures of actual UHF RFID technology in terms of tag sensitivity, standards and regulations (see ISO Standards 2007; ETSI, 2007a; ETSI, 2007b; ETSI, 2007c; IDA, 2008; FCC, 2007; SRRC, 2007). Based on these and on the following information, system integrators should have the ability to perform a proper RFID systems characterization and performance analysis.

2. Interrogation zone sensing

Interrogation zone sensing is a key process not only essential for the preparation of human visible data which give us a general picture of the actual performance level but is also important for computer aided analysis to determine improvement potentials and to define proper optimization strategies.

2.1 Sensing devices

In fact, it is not easy to determine the field strength in consideration of multi-path propagation within the relevant gate or portal area analytically. A better approach to this problem is not only the utilization of statistical models that are already successfully used to describe field propagation effects and indoor radio propagation channels (see Rappaport & McGillem, 1989), but also the use of ray tracing methods (see Bosselmann & Rembold 2006a; Bosselmann & Rembold 2006b) to simulate the field distribution in passive UHF RFID applications.

However, all these models require an extensive study of the actual field distribution obtained from the results of the measurement data analysis. For instance, the characterization of the field strength distribution inside a typical portal application in combination with different arrangements of tagged items on a pallet requires a complex measuring system. The measurement equipment should fulfil specific requirements. First, it should be neutral to the ambient conditions in order that the field distribution is not affected by the measurement setup itself. As second requirement, it should be capable to measuring the field characteristics along tag moving trajectories, on tag positions and optionally in the pallet for a better comparison to the actual available tag power. Repeatability should also be ensured in order to align all measurement data properly.

There are several measurement devices presented in the literature which are suitable for interrogation zone sensing. An interesting measurement device is proposed that allows the determination of the field strength on and inside individual pallets (see Redemske & Fletcher, 2005). This device operates as a battery powered active “tag emulator” and is part of the inventory and anti-collision process of the interrogator. Therefore, multiple sensor modules can be operated simultaneously. The individual field strength measurements are encoded in the EPC number (see ISO Standards, 2007), which is requested by an interrogator during the inventory process. This characteristic enables a wireless transmission of the measurement result. Another more sophisticated measurement devise (see CISC, 2006), also

suitable for interrogation zone sensing, allows high-speed continuous data sampling of several sensor modules mounted along a specified moving direction, when triggered and moved through a gate for instance. Unfortunately, these devices suffer from additional drawbacks, on the one hand, the complicated cabling of sensor modules and main controller makes the handling difficult, on the other hand, the dipole measurement antenna is sensitive to material properties and may influences the measurement accuracy, especially in setups where the field strength inside pallets is of particular interest. As mentioned already in the introduction, J. Mitsugi et al., have already published a similar mobile field recorder for UHF RFID interrogation area measurement (see Mitsugi & Tokumasu, 2008).
For system integrators or non-professionals, it is very important to have a low-cost and easy to handle measurement device available. Furthermore, the measurement device should feature comparable size and shape of standard tags in order to be placed on real tag positions and to be operated on similar trajectories.
We have adopted these ideas and have designed and developed two contactless battery powered measurement devices. One of which is equipped with a dipole based field probe and is more suitable for free space field strength measurement and the other one equipped with a loop based field probe antenna which is more insensitive to different material properties for measurements inside pallets. See a photograph of these devices in Fig. 1 for detail.

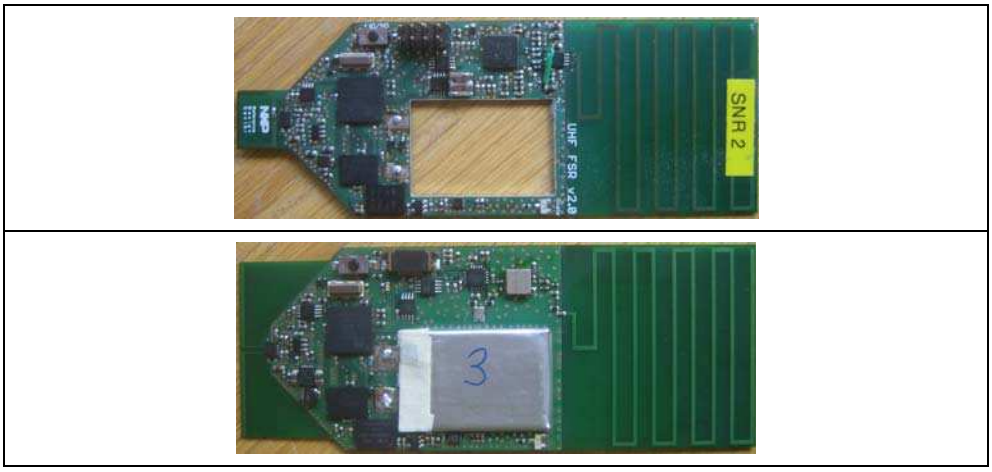

Fig. 1. Photograph of NXP mobile field strength recorders. One of which equipped with dipole-antenna based field probe and the other with loop-antenna field probe

2.2 Test environments

UHF RFID gates and portals are deployed in deferent geographical regions operating under different local regulations. In open loop applications, goods are transported from one country to others passing different types of gates, but normally only with an individual tag attached during its production or packing process. Therefore, it is important that all gates, doors and portals have a standard shape in order to fulfil system reliability along the entire supply chain. In this context we propose a novel characterization method of UHF RFID portals based on RF field strength recording, RFID tag channel modeling, and qualification

according to the derived channel model. This method can also be extended to doors, portals or other high power UHF RFID applications with comparable characteristics.
Two basic principles of the measurement procedure for portal interrogation zone sensing are illustrated in figure 2 and figure 3.

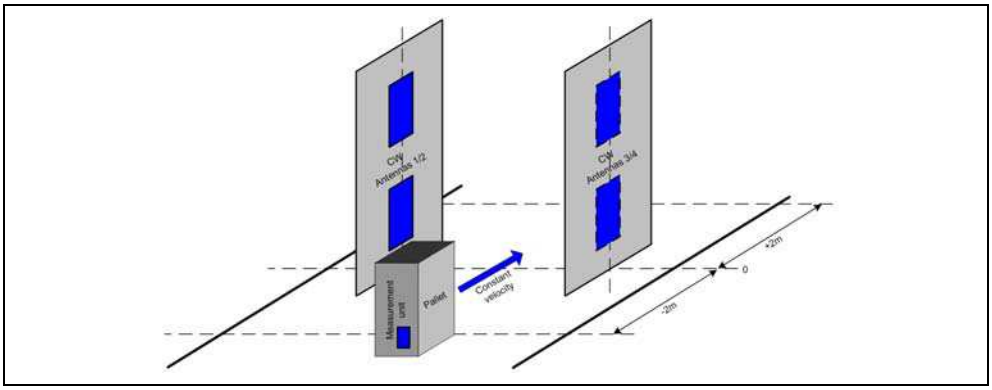

Fig. 2. Laboratory setup for interrogation zone sensing. The pallet under test is passed through the portal with constant velocity by using an automated transport system

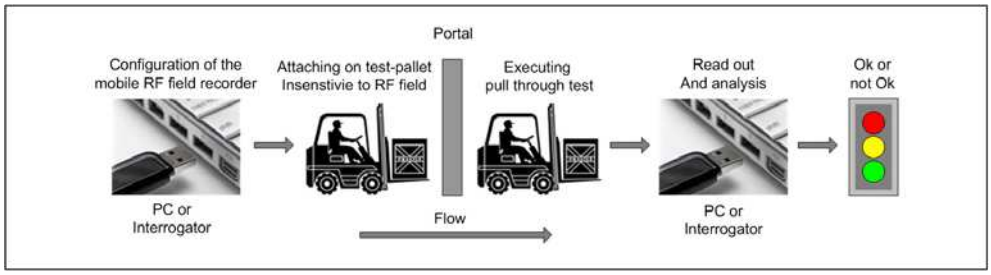

Fig. 3. Direct test in industrial environments. The FSRs are configured by a PC or interrogator, attached and passed through the portal. Later measurement data analysis gives information about portal quality .

In principle, there are three possibilities to perform interrogation zone measurements. One is a setup under test operated in a controlled environment. An experimental study that addresses the readability degradation in UHF RFID systems within an anechoic chamber is proposed in (Mitsugi & Hada, 2006). Such a setup is only useful to identify base performance and to use the measurement data as a reference to real-life environments since the influence of field propagation cannot be determined properly. Comparable real-life conditions can be achieved within a laboratory environment which refers as second possibility of evaluation. In section 3, the results of an application specific study of a passive UHF RFID system examined under laboratory conditions is presented. Furthermore, a direct test in industrial environments should be fast and reliable. One evaluation procedure for RFID portals can be as illustrated in figure 3. The presented FSR is specifically suitable for this kind of application tests. Once the FSR is configured by an interrogator or PC it can be attached or integrated in a pallet under test, triggered and moved through the gate. This operation is repeated several times depending on the number of FSR simultaneously used

and to increase the accuracy of classification. In section 4, a model based classification method for RFID portals is presented.

3. Probability of interrogation degradation

Different application tests have shown that material properties of the tagged items, beam-width and quantity of the interrogator's transmit antennas, tag sensitivity and position of the tag have significant impact on the occurrence of missing reads. This study addresses also the influence of the pallet density and its absorption characterizes with respect to the electromagnetic wave propagation effects on field coverage and readability. All measurements were managed within a laboratory environment with the help of an automatic transportation device of pallets to ensure repeatable measurement conditions. The test portal was a replica of a typical portal used in a distribution centre (DC) within a real-life RF-environment.

3.1 Portal and pallet setups

The portal consists of two chambers that are 3m apart, each containing two circular-polarized interrogator antennas, the pallets are setup using three individual arrangements of items are chosen.

3.1.1 Pallet setup A

Setup A (see figure 4) is a type of skeleton pallet that is used to determine the field strength in a quasi free-space environment inside the portal area. A set of 45 sensor modules at different locations on the skeleton pallet are used to measure the field strength along the moving path through the portal. The portal area is restricted to ±2m from the antenna symmetry axis by definition (see figure 2). Previous measurements had shown that regions outside this area are not relevant for the interrogation zone analysis since the RF power levels outside are below the sensitivity threshold of typical tags.

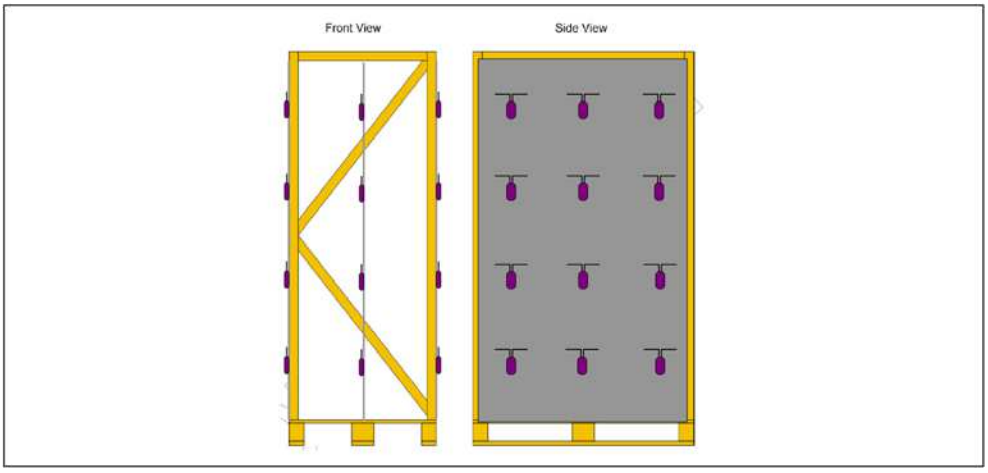

Fig. 4. Wooden skeleton pallet equipped with sensor modules for quasi free-space field strength analysis inside the portal area.

3.1.2 Pallet setups B and C

Setups B and C are sub-sets of the pallet arrangement illustrated in figure 5, indexed as pallet A and B, respectively. Pallet A consists of coffee packs, soap and liquids, whereas pallet B consists of toilet paper, chocolate bars and swaddling bands.

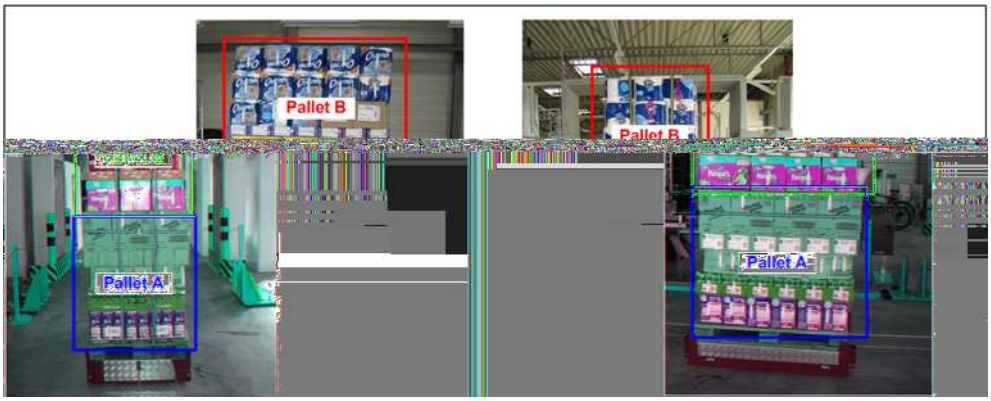

Fig. 5. Pallet with typical items often transported in a supply chain (mineral water, fish, toilet paper, toys and snacks) placed on the automated transport system

3.1.3 Pallet setup D

Setup D (see figure 6) consists of typical items that are often transported in a supply chain like mineral water, fish, toilet paper, toys and snacks. The alignment of the 45 sensor modules is similar to all previous setups.

Fig. 6. Pallet with typical items often transported in a supply chain (mineral water, fish, toilet paper, toys and snacks)

3.2 Measurement analysis

As already mentioned, the test portal consists of four interrogator antennas (Intermec IA39B) at distinct positions. Only one antenna is active during one test scenario of all listed pallets. This corresponds to the regular operation of common interrogators since there is just one RF transmitter integrated and all the attached antennas to it are multiplexed in time. The operating frequency was chosen in the European UHF RFID frequency band at channel 4 (867.5MHz) and the power level was set to the maximum permitted value of $2W_{ERP}$ for the entire measurement period. One measurement cycle consists of the following procedure.

First, the selected pallet was equipped with the sensor modules at well-defined locations on the items, where normally the tags are placed, and the pallet under test was placed on the automatic transportation device afterwards. In the second step, the selected pallet was automatically triggered and moved back and forth with constant velocity of v_0=0.544m/s to ensure measurement repeatability. The chosen velocity is a trade-off between maximum sampling rate of the field recorder and spatial resolution along the moving direction. In the final step, the average of five runs at every single sensor module position was calculated and used for further measurement analysis.

3.3 Measurement results

The field characteristics of two sensor modules of pallet setup A associated with the defined moving path through the portal and with antenna 1 as power source are illustrated in figure 7a. The characteristic of module 40 shows a significant peak in the centre of the portal. In contrary, module 44 shows a flat distribution overlaid by some degree of interference.

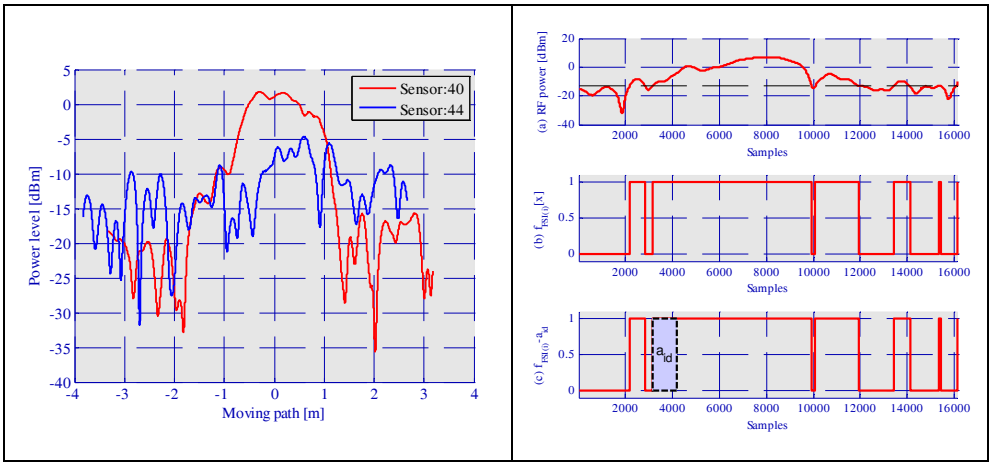

Fig. 7. (a) Field characteristics of two sensor modules of pallet setup A associated with the defined moving path through the portal and (b) graphical representation of the basic calculations used for field coverage and readability associated with a specified sensitivity threshold of -13dBm; the influence of a_{id} is illustrated at only one piecewise constant region for clarification

In general, missing reads will occur when the available power level is lower than the sensitivity threshold of the tag. For this reason, we propose to introduce two quality factors for gates and pallets defined as readability and field-coverage associated with a dedicated section or read zone of the maximum portal area. The readability represents a quality indicator for a dynamic environment and field-coverage for a static environment, respectively. We note that the expected readability and field coverage obtained in one section are identical for a static environment. These indicators are defined as follows:

3.4 Field-coverage definition

First, we define a field strength indicator function $f_{FSI}[x]$ as:

$$f_{FSI(i)}[x] = \begin{cases} 1, \text{for } p_i[x] \geq s_{th} \\ 0, \text{for } p_i[x] < s_{th} \end{cases}, s_0 \leq x \leq s_1. \quad (1)$$

Where $p_i[x]$ are the field strength measurement samples along the moving path of the i-th sensor module, s_{th} represents the sensitivity threshold of the tag, and s_0, s_1 define the section boundaries on the moving direction and it holds that $s_1 > s_0$. The sensor boundaries are related to the valid interrogation zone. All the measurements were taken from the four interrogator antennas independently without varying the positions of the sensor modules. Therefore, we have to distinguish between four different sample sets recorded from every single module. The RF power levels measured depend on the effective distance between the sensor modules and the distinct interrogator antennas. In order to obtain the maximum field coverage, $p_i[x]$ is the set chosen, which produces the maximum on average power distribution along the moving direction generated by the individual interrogator antennas. This corresponds to the minimum effective distance from the individual sensor module to the operating interrogator antenna. In reference to the portal application, this is an issue of antenna switching strategy and this is not addressed in this context. However, this selection is comparable to the optimum powering conditions for the individual tags located at these sensor module positions.
Whereas, the field-coverage of a dedicated section or read zone is defined as:

$$I_{FC} = \frac{1}{N(s_1 - s_0)} \sum_{i=1}^{N} \sum_{x=s_0}^{s_1} f_{FSI(i)}[x] \quad (2)$$

Where N represents the number of sensor modules, s_1-s_0 describes the dedicated section boundary of the portal area associated with the moving direction in one dimension.

3.5 Readability definition

For the determination of the readability in a dynamic environment, additional parameters are required. One parameter is the inventory duration of a signal tag. For instance, if we rely on the ISO 18000-6C standard (see ISO Standards, 2007), this inventory duration requires on average 6ms in a dense interrogator environment. Furthermore, the moving speed of the pallet and the back-up lifetime of the tag after power loss are required, whereas the back-up duration can be neglected in this context, since this period is normally shorter than several μs and lies below the resolution of the field recorder used.
The readability of one single tag is defined as:

$$I_{RA(i)} = \sum_{j=1}^{M_i} \max\left[0, \sum_{x=n_{j0}}^{n_{j1}} f_{FSI(i)}[x] - a_{id}\right], \quad (3)$$

and the expected readability in a dedicated read zone is defined as the average readability calculated on the basis of the individual results:

$$I_{RA} = \frac{1}{N} \sum_{i=1}^{N} I_{RA(i)}. \quad (4)$$

Where n_{j0} and n_{j1} are the lower and upper bounds of the j-th piecewise constant region of $f_{FSI(i)}[x]=1$ within the section boundaries. M_i is the number of piecewise constant regions inside the section boundaries, N represents the number of sensor modules, a_{id} denotes the required field coverage for one tag inventory cycle during the moving of the pallet through the portal in a dynamic scenario which is defined as:

$$a_{id} = \left\lceil v_0 t_{id} n_{spm} \right\rceil. \tag{5}$$

Where v_0 is the moving velocity of the pallet through the portal, t_{id} represents the inventory duration and n_{spm} denotes the number of measurement samples per meter. See figure 7b for clarification.

3.6 Field coverage results

If we refer to figure 8a, we can see that the field coverage is nearly identical for the given sensitivity thresholds within the section boundaries ±0.5m in reference to the portal centre. If we consider the section boundaries ±1.5m, we can determine a field coverage reduction of about 8% when the sensitivity threshold of the tag is increased from -15dBm to -13dBm. These values correspond to sensitivity values of current commercial tags. That means, if the interrogator is triggered at these specified section boundaries, the probability of a successful inventory will decrease by 8% in a static (no motion) free space environment in consideration of multi-path propagation (pallet setup A).

The comparison of all specified pallet configurations at sensitivity thresholds -13dBm and -15dBm leads to the following results. It can be shown that the field coverage associated with the section boundaries measured in all specified pallet configurations has an equal tendency with different offsets mainly caused by the damping properties of the items on the pallet (see figure 8b). This damping characteristic is investigated in (Fletcher & Marti, 2005) by using fundamental electro-magnetic propagation principles. For instance, setup B leads to a field coverage of about 80% in the section boundaries ±0.5m whereas setup D achieves 86% coverage and setup C achieves 92% coverage.

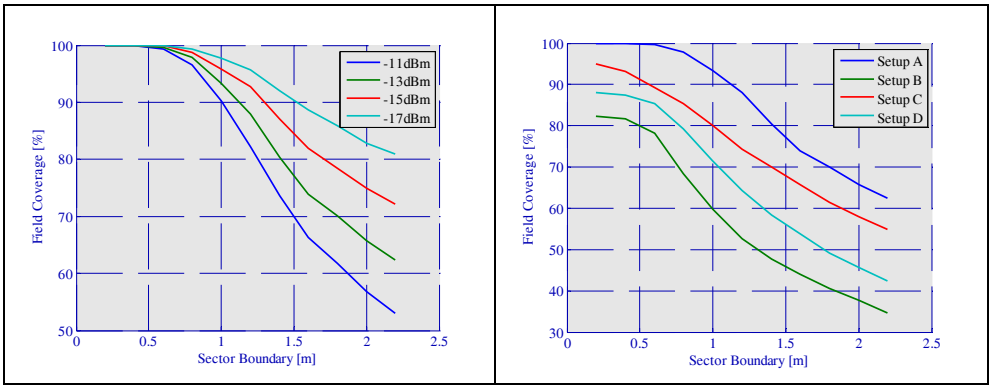

Fig. 8. (a) Field coverage associated with the dedicated section boundaries dependent of different tag sensitivity thresholds (-11, -13, -15, and -17dBm) based on the pallet setup A (free-space portal area); (b) Field coverage associated with the dedicated section boundaries of all specified pallet configurations based on a sensitivity threshold of -13dBm

The reflection characteristics of the electro-magnetic waves on and inside different pallets are independent of the material properties according to the measurement results. In contrary, the absorption characteristics depend significantly on the material properties. This means that the radiated RF power absorption by the items on the pallet and not the random multi-path interference causes reading performance degradation. A reduction of the sensitivity threshold from -13dBm to -15dBm (see figure 9a) is leading to a slight improvement of the field coverage. The probability of inventory increases by 2.5% in pallet setup B, by 3.5% in pallet setup C and by 3% in pallet setup D. If the read zone is expanded up to the gate boundaries, the relative field coverage will increase but will not exceed 10% in all configurations.

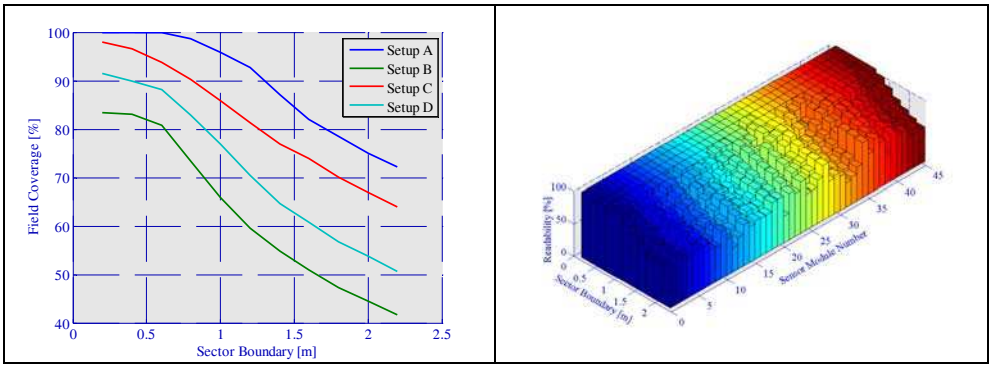

Fig. 9. (a) Field coverage associated with the dedicated section boundaries of all specified pallet configurations based on a sensitivity threshold of -15dBm; (b) Readability at the position of all sensor modules of pallet setup A (free space) with a sensitivity threshold of -13dBm associated with the dedicated section boundaries (read zones)

In conclusion, a reduction of the sensitivity threshold will increase the field coverage insignificantly in comparison to the absolute field coverage in the specified interrogation zone. The analysis has shown that the field coverage is less than 100% except in a free-space environment (setup A) and can lead to missing reads in all other configurations. Consequently, there is no optimum inventory optimization feasible, because it is nearly impossible to estimate the tag population, which is actually powered by the interrogator in order to set the optimum slot-count value for anti-collision resolution according to (ISO Standards, 2007). A trial-and-error polling technique that uses the collision rate as parameter would be the most promising approach to reduce the number of missing reads.

3.7 Readability results

The readability of pallet setup A with a sensitivity threshold of -13dBm is illustrated in figure 9b. It can be shown that all sensor modules are readable with 100% confidence in the section boundaries ±0.5m. The expected readability decreases on average by 60% when the section boundaries are set to ±2.2m. This characteristic is mainly caused by lower field coverage outside the portal centre and is a consequence of higher path-loss of the electromagnetic energy. This means, when the interrogator is triggered at these section boundaries, the probability of field coverage of on particular tag along its moving direction is lower. Therefore, the readability of tags decreases in combination with the random occurrence of its inventory instant inside the specified interrogation zone.

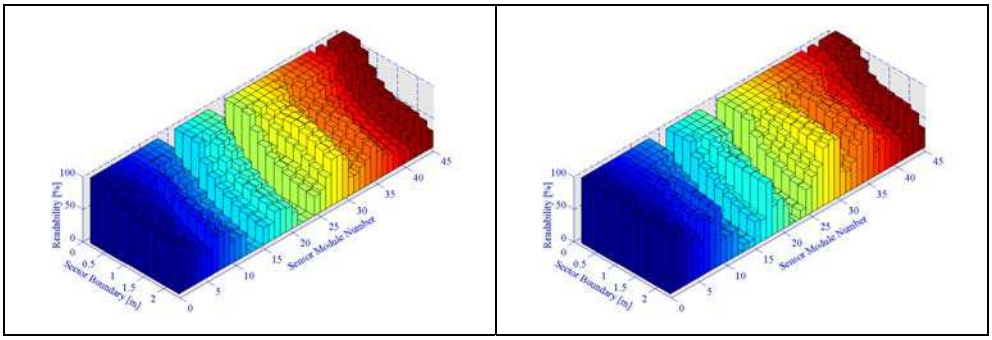

Fig. 10. (a) Readability at the position of all sensor modules of pallet setup B with a sensitivity threshold of (a) -13dBm and (b) -15dBm associated with the dedicated section boundaries (read zones)

The readability of tags is not ensured at several sensor module positions in pallet setup B (see figure 10a). The power levels at the sensor module positions 13, 14, 15, 22, 23, 24, 40, and 42 are permanently below the sensitivity threshold of –13dBm and tags attached to those particular items cannot be read in any case. This behaviour is mainly caused by the absorption characteristic of items, especially water or metal food casings, arranged in the line-of-sight direction to the operating interrogator antenna. For instance, when the sensitivity threshold is reduced from -13dBm to -15dBm the readability at sensor module positions 14, 15, 22, 24 and 42 can be achieved, but the readability is still not achievable at the positions of the remaining three modules 13, 23 and 40 (see figure 10b).
In conclusion, the readability of all other pallet configurations showed comparable results. The readability is critical at positions where metal food casings are in the line-of-sight direction to the powering antenna. A sensitivity threshold reduction helps to overcome the powering problem at certain positions, but under some extreme conditions, the readability is still not achievable.

4. Interrogation zone characterization

Basically, it is not possible to accomplish an interrogation zone characterization of all significant pallet configurations involved in terms of known performance degradations factors. Instead we propose a method that requires only free space measurement data recorded in the appropriate interrogation zone. This data is correlated with an RFID tag channel model valid for portal applications to determine a statistical value of the expected field coverage within the interrogation zone. An additional safety margin between supposed tag sensitivity and expected field coverage ensures the readability of pallets carrying items with high RF absorption characteristics. The safety margin will come out from experimental test in real life portal application and will be treated as an additional loss added to the free space path-loss model.

4.1 Statistical modeling of the interrogator-to-tag powering channel

The primary goal of the channel modeling is to identify the fading characteristics of the interrogator-to-tag energy transfer along a typical trajectory through the portal and to determine the mean path loss on the portal cross-section. Many of these channel modeling

approaches are based on the evaluation of the probability or cumulative density function (CDF) of the transfer signal amplitude over time. Rappaport (see Rappaport & McGillem, 1989) can be mentioned for his pioneering work in the research of UHF signal fading characteristics in factory environments. During the investigation of UHF cellular radio a variety of different channel models were propose for distinct indoor or outdoor scenarios (see Nikookar & Hashemi, 1993; Hashemi, 1993). These channel models are not directly applicable to UHF RFID due to its heterogeneous mode of operation. Little research is carried out in this area so far. What is already published are channel models dealing with short range indoor applications (see Mayer et al., 2006) or statements that a Rician distribution fits UHF RFID applications (see Kim et al., 2003) because of its strong line-of-sight mode of operation. But this assumption is not always valid because tags are not only attached on the pallet surface. It is not promising to apply a statistical channel model to the entire read volume since tag trajectories and power density are not considered properly. Therefore, we propose a two step approach leading to a general channel model for portal applications. The basic idea is illustrated in figure 11a. The read volume is divided into two orthogonal planes defined as TAG-plane and LOS-plane. The TAG-plane is aligned to the tag moving path through the portal, perpendicular to the interrogation antennas, and is associated with a signal amplitude fading model and the LOS-plane is aligned to the mean power distribution of the cross-section in the centre of the gate associated with an appropriate path-loss model. Measurements have shown that the path-loss along the LOS-plane has a significant impact on the mean power distribution.

4.1.1 TAG plane fading model

Once the tag is moving through the portal along the TAG-plane, it will pass a RF power distribution comparable to a characteristic illustrated in figure 7a. A statistical probability density function of such characteristic can be modelled by means of a bimodal distribution function.

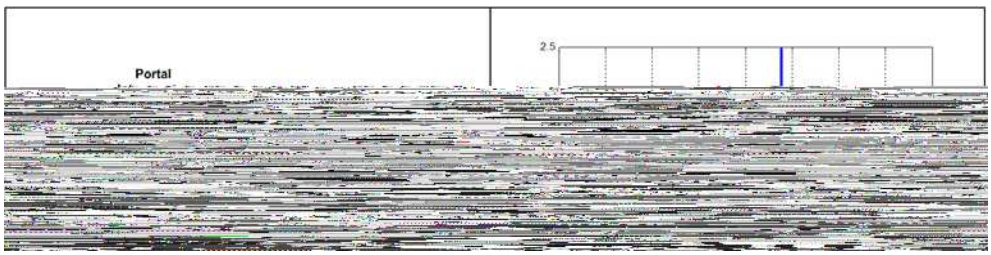

Fig. 11. (a) Two step approach to a portal channel model. TAG-plane is aligned in tag moving trajectory providing field coverage distribution and the LOS-plane is aligned to the portal cross-section for maximum mean power distribution modeling and (b) Bimodal RF power level probability distribution of one continuous measurement along a typical tag trajectory through the portal

The strong line-of-sight component occurring in the centre of the gate is modelled with a log-normal distribution and the fading components outside the portal centre are modelled with a normal distribution function. The general bimodal distribution function can be expressed with:

$$F_{bm}(x) = pF_1(x) + (1-p)F_2(x), \tag{6}$$

where p is the fraction of the deferent distribution functions $F_1(x)$ and $F_2(x)$. When we expand (6) with the defined distribution functions, we get the proposed statistical fading model for the TAG-plane as:

$$F_{TAG}(x) = \begin{cases} p\dfrac{1}{\sigma_1\sqrt{2\pi}x}\mathrm{e}^{-\frac{(\ln x-\mu_1)^2}{2\sigma_1^2}} + \\ +(1-p)\dfrac{1}{\sigma_2\sqrt{2\pi}}\mathrm{e}^{-\frac{(x-\mu_2)^2}{2\sigma_2^2}} & x>0 \\ 0 & x\le 0 \end{cases} \tag{7}$$

For example, fitting this distribution model to the amplitude fading characteristic illustrated in figure 11b yields values p=0.256, μ1=1.790, σ1=1.929, μ2=0.416, σ2=0.111, and scaling factor sc=0.327. The scaling factor is only important for the nonlinear least square fitting algorithm and has no influence on the cumulative distribution function that indicates probability of signal strength lower a specified threshold.

4.1.2 LOS-plane mean power model

The LOS-plane mean power model describes the expected mean power level of the cross-section in the centre of the portal. This model consists of a general path-loss model and a multi-ray interference model. General path-loss models are described in (Rappaport, 2002; Leong et al., 2006), but the Friis transmission equation (8) is used for the present problem formulation.

$$P_r = P_t G_t g_r \left(\frac{\lambda}{4\pi r}\right)^2, \tag{8}$$

where P_t is the transmitted power, G_t is the gain of the interrogation antenna, g_r is the gain of the tag antenna, λ represents wavelength of the carrier and r is the distance to the target point. On the other hand, the multi-ray interference model considers first order ground reflections and the total reflection property of the opposite portal chamber. The first order ground reflections are modelled by means of the well known Fresnel's reflection coefficients (9) valid for an interface between air and ground.

$$\rho_h = \frac{\cos\phi - \sqrt{n^2-\sin^2\phi}}{\cos\phi + \sqrt{n^2-\sin^2\phi}}, \quad \rho_v = \frac{n^2\cos\phi - \sqrt{n^2-\sin^2\phi}}{n^2\cos\phi + \sqrt{n^2-\sin^2\phi}}, \tag{9}$$
$$\rho_c = \frac{\rho_h + \rho_v}{2},$$

where, ρ_h, ρ_v, ρ_c represent perpendicular, parallel and circular incidence of the electric field, n is the complex refractive index of concrete and Φ is the angle of incidence. The thickness of the concrete ground is taken into account according to (Sato et al., 1996). The total reflection property of the opposite portal chamber has its impact only on the free-space measurement scenario. Once passing a pallet through the gate, the line-of-sight direction is blocked and most of the energy is absorbed or reflected by the pallet. We have set up a measurement procedure to identify the absorption characteristics by detection of the S_{21} scattering parameter using a network analyzer and opposite antenna pairs.
In many cases, the opposite chamber is made of metal plates without shielding in order to achieve robustness and cost efficiency. This property must be considered during the qualification procedure since the measured power levels in an empty portal are higher due to the virtual gain of the opposite chamber. We propose to model the reflection property according to the behaviour of a flat metal plate with dimensions of the chamber outline. This is just a rough estimation that accounts for the worst-case scenario and provides maximum safety margin with respect to the normal case of operation. The reflection property of a metal plate can be described with the well-known monostatic radar cross section (RCS) formula (10). This approach is also used for indoor radio channel modeling (see Kajiwara, 2000; Fenn & Lutz, 1993) and to determine a theoretical RCS value dependent on the incidence angle (see Ross, 1966).

$$G_r = \frac{\sigma_{RCS}}{4\pi d_p^2}, \quad \sigma_{RCS} = \frac{4\pi A^2}{\lambda^2}, \tag{10}$$

where, G_r is the equivalent gain, σ_{RCS} is the monostatic RCS, d_p is the portal width, A is the equivalent are of the chamber and λ is the wave length of the power carrier. Finally, we define a similar UHF RFID radio channel model as proposed in (Han et el., 2004).

$$P_r = P_t g_r \left(\frac{\lambda}{4\pi}\right)^2 \left| \sqrt{G_t(\vartheta_0)} \frac{1}{r_0} \mathrm{e}^{-jkr_0} + \sqrt{G_t(\vartheta_1)} \rho_c \frac{1}{r_1} \mathrm{e}^{-jkr_1} + \sqrt{G_r} \frac{1}{r_2} \mathrm{e}^{-jkr_2} \right|^2, \tag{11}$$

where P_r is the power level at the target point, P_t is the transmit power of the interrogator, λ is the wave length of the power carrier, $G_t(\vartheta_{0,1})$ is the appropriate interrogation antenna gain dependent on the E-plane angle, $r_{0,1,2}$ represents path length.

4.1.3 Joint TAG/LOS model

In order to obtain a 3D model that covers the desired interrogation zone, we propose the following approach. The TAG plane fading model describes the statistical distribution of the signal amplitude without contribution to the signal level. Referring to figures 7 and 12, the maximum value of the signal amplitude will be different at different tag locations and when the mean distribution is fitted over all tag locations, all the individual signal level distributions result in one CDF associated with the overall tag readability. In contrast, the LOS plane mean power model gives a value for the maximum signal value in the portal cross section and defines the abscissa maximum of the tag readability CDF. The abscissa minimum is defined by the resolution of the FSR, equal to -40dBm. Finally, the tag readability is obtained by application of a dedicated tag sensitivity threshold.

4.2 Results and pallet readability

We apply this approach to two different portal setups, one is operated according to EU (European) and the other according to US regulations. The EU setup consists of four individual Kathrein 25-180 circularly polarized directional antennas, 10.5 dBic, 70° H-plane 3dB-beamwidth and 30° E-plane beam width, arranged in [0.7, 1.4, 1.4, 0.7] meters from ground plus a Sirit Infinity 510 UHF RFID interrogator set to 27 dBm conductive power, 866 MHz, and continuous wave output. The US setup consists of 4 individual Symbol Andrew RFID-900-SC high performance area antennas, 6.0 dBi, 70° in both H and E-plane 3dB-beamwidth, arranged in [0.65, 1.75, 1.75, 0.65] meters and the Sirit Infinity 510 set to 27 dBm conductive power, 915 MHz, and continuous wave output.

4.2.1 TAG plane fading model results

According to the proposed method, the TAG-plane measurements are accomplished by means of the FSR devices. A set of 18 measurements where taken per antenna. Therefore, the FSR position is varied in dimensions of a typical pallet outline and moved through the portal under test utilizing an automated transportation device (see Muehlmann & Witschnig, 2007). The CDFs derived from the measurement data show similar characteristics and do not depend on the antenna position (see figure 12). Hence, it can be concluded that the portal interrogation zone does not depend on the portal surroundings. It can be noted, that the free space field coverage is a bit higher in the US setup, 50% achieved at around -10 dBm compared to -15dBm achieved in the EU setup. This is probably caused by the broader antenna beam width used in the US setup (the broader beam width combined with scattering from metal object surrounding thus the portal may generate a higher level of reflections and resulting in an increasing of the field).

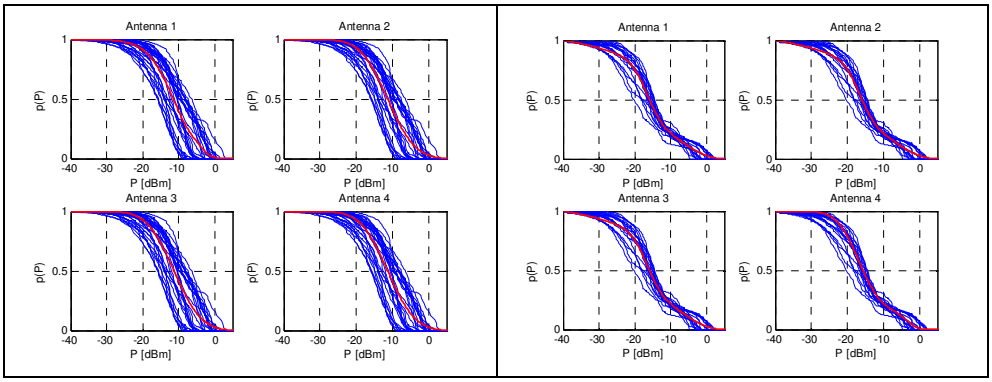

Fig. 12. (a) CDF of the used US portal derived from the FSM measurements and fitted model function showing p(P) as probability of power level greater a threshold and (b) CDF of the used EU portal derived from the FSM measurements and fitted model function showing p(P) as probability of power level greater a threshold.

4.2.2 LOS-plane mean power model results

According to the proposed method, the LOS-plane mean power model is used to describe the field strength distribution on the portal cross-section. Figure 13a shows the simulation result of the EU setup where antenna 3 is the interrogation antenna and which defines the x-axes origin. The simulation result matches well to the real life situation. The comparison is

performed by taking the field strength values of the TAG-plane measurement data when the FSM is passing through the portal cross-section. The US setup is analyzed in an equal manner. The simulation result is illustrated in figure 13b and shows a slightly lower mean power distribution compared to the EU setup.

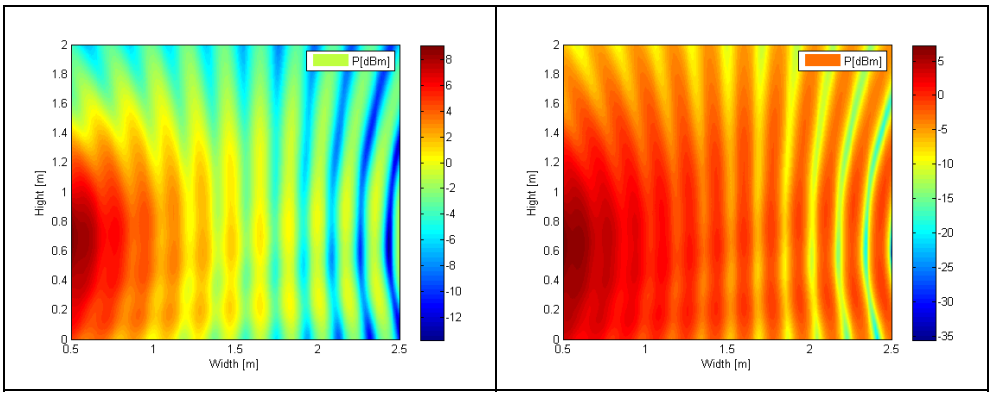

Fig. 13. (a) LOS-plane mean power model of the EU portal setup. Antenna 3 is used as interrogation antenna and defines the x-axes (vertical) origin and (b) LOS-plane mean power model of the US portal setup. Antenna 3 is used as interrogation antenna and defines the x-axes origin

4.2.3 Pallet readability

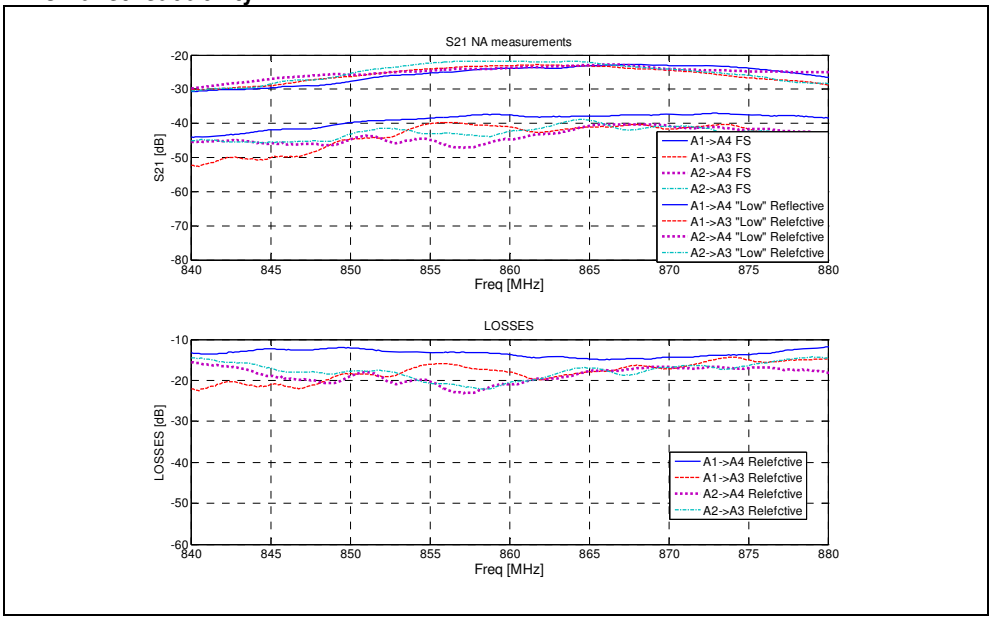

Fig. 14. S_{21} measurement results of a pallet with dimensions 1.2m x 1.4m x 2.2m by using opposite antenna pairs for radiation and reception. A network analyzer is used to determine S_{21} versus frequency.

The pallet readability depends not only on the prevalent field coverage of the interrogation zone and the pallet density but also on the operational sequence of the anti-collision protocol (see ISO Standards, 2007). There has been extensive research carried out in the optimization of such ALOHA anti-collision protocols (see Jin et al., 2007; Floerkemeier & Wille, 2006; Vogt, 2002; Wang & Liu, 2006) which impact on the reading performance is beyond the scope of this study. A practical test of these two portals with a pallet (1.2m,1.4m,2.2m) containing 200 tagged items (see figure 5) has shown that the EU portal setup reaches 86.8% read-rate whereas the US portal setup 80%. Referring to figure 13, the mean LOS power level is about 2dB higher in the EU compared to the US setup which explains the different read-rates. The pallet loss characteristic was measured and illustrated in figure 14b. Assuming a linear path-loss through the portal and that all four antennas are in the interrogation sequence involved, a path loss of -11dB can be expected from the pallet outline to its centre.

5. Conclusion

Two quality factors for gate and portal applications are proposed in this text, which are defined as field coverage and readability. Both indicators are in reference to the dedicated interrogation zone specified as sections with defined boundaries on the pallet moving path. The expected field coverage of different setups has similar tendency associated with the section boundaries and depends on the damping characteristics of the different pallet configurations and on the sensitivity threshold of the tag. It can be enhanced up to 10% by increasing the sensitivity from -13dBm to -15dBm. However, the sensitivity improvement is insufficient in reference to the absolute field coverage that is achieved in particular pallet arrangements. In contrary, the readability of tags at particular positions can be achieved by increasing their sensitivity.

The readability as well as the field coverage depends on the section boundaries. The closer the section boundaries to the centre of the gate the higher the expected field coverage and readability will be. This characteristic is mainly caused by the gain pattern of the interrogator antenna, which shows normally a dominant main lobe in the direction to the portal centre.

The probability of missing reads from the perspective of field coverage and readability can be reduced by defining the appropriate interrogator triggering position in combination with the main lobe of the interrogator antennas on the one hand. On the other hand, the improvement of the tag sensitivity will lead to higher readability and increases the probability of a successful inventory accordingly. However, this experimental study has shown that the readability is not guaranteed at certain positions on the pallet with state of the art technology, where extreme conditions prevent the activation of the affected tags.

The sensitivity enhancement up to a certain level must be investigated properly. Therefore, two conflicting factors that influence the overall system performance must be considered. These factors are the receiver sensitivity and dynamic range of the interrogator and the occurrence of unwanted reads in close proximity.

In conclusion, a novel interrogator-to-tag channel model has been presented that describes the field strength distribution in the portal interrogation zone. The model parameters are derived from the measurement data and a custom-made FSR is used to determine the actual field strength along typical tag trajectories.

Further investigations are needed on how to interpret the model parameters p, μ_1, σ_1, μ_2, and σ_2 with respect to an optimization of the portal setup, beam-width and selection of the antenna, etc. Furthermore, the reflection characteristic of the opposite chamber needs to be studied in different setups to derive general numbers. Based on the LOS-model it should be possible to predict this reflection characteristic out of the measurement data. In order to predict the read-rate out of the model parameters, it is essential to know absorption and reflection figures of possible pallet configurations as well as actual tag locations on the tagged items. These parameters are mainly customer related and no work to this subject is presented in this text accordingly. In addition, it is essential to incorporate the influence of the anti-collision algorithm in order to make a statement about the overall read-rate.

6. References

Aroor, S. R. & Deavours, D. D. (2007). Evaluation of the State of Passive UHF RFID: An Experimental Approach. *IEEE Systems Journal*, vol 1(2), December 2007, pages 168-176

Bosselmann, P. & Rembold, B. (2006a). Ray Tracing Simulations for UHF Passive RFID Applications, *15th IST Mobile and Wireless Communications Summit*, Mykonos, Greece, 4-8 June 2006

Bosselmann, P. & Rembold, B. (2006b). Ray Tracing Method for System Planning and Analysis of UHF-RFID Applications With Passive Transponders, *2nd ITG/VDE Workshop on RFID*, Erlangen, Germany, 4-5 July

CISC. (2006). RFID Field Recorder R 1.0, www.cisc.at.

De Vita, G. & Iannaccone, G. (2005). Design Criteria for the RF Section of UHF and Microwave Passive RFID Transponders, *IEEE Transactions on Microwave Theory and Techniques*, vol. 53, No. 9, September 2005, pages 2978-2990

ETSI. (2007a). European Telecommunications Standards Institute (ETSI), EN 300 220 (all parts): Electromagnetic compatibility 2007 EPCglobal Inc. Page 6 of 41, 11 June 2007, and Radio spectrum Matters (ERM); Short Range Devices (SRD); Radio equipment to be used in the 25 MHz to 1000 MHz frequency range with power levels ranging up to 500 mW

ETSI. (2007b). European Telecommunications Standards Institute (ETSI), EN 302 208: Electromagnetic compatibility and radio spectrum matters (ERM) – Radio-frequency identification equipment operating in the band 865 MHz to 868 MHz with power levels up to 2 W, Part 1 – Technical characteristics and test methods

ETSI. (2007c). European Telecommunications Standards Institute (ETSI), EN 302 208: Electromagnetic compatibility and radio spectrum matters (ERM) – Radio-frequency identification equipment operating in the band 865 MHz to 868 MHz with power levels up to 2 W, Part 2 – Harmonized EN under article 3.2 of the R&TTE directive

FCC. (2007). Federal communication commission, Radio Frequency Devices Intentional Radiators, Radiated emission limits, general requirements, Part 15 Subpart C, § 15.245, 15.246, 15.247

Fenn, A. J. & Lutz, J. E. (1993). Bistatic radar cross section for a perfectly conducting rhombus-shaped flat plate: simulations and measurements, *IEEE transactions on antennas and propagation*, vol. 41, pages 47-51

Finkenzeller, K. (1999). *RFID Handbook: Fundamentals and Applications in Contactless Smart Cards and Identification*, 2nd ed. New York: Wiley

Fletcher, R.; Marti, U.P. & Redemske, R. (2005). Study of UHF RFID Signal Propagation through Complex Media, *IEEE Antennas and Propagations Society International Symposium*, vol. 1B, July 2005, pages 747-750

Floerkemeier, C. & Wille, M. (2006). Comparison of transmission schemes for framed ALOHA based RFID protocols, *Applications and the Internet Workshops, 2006. SAINT Workshops 2006, International Symposium on*, Jan. 2006, pages 23-27

Glidden, R. & Schroeter, J. (2005). Bringing long-range UHF RFID tags into mainstream supply-chain applications, *RFDESIGN, RF and Microwave Technology for Design Engineers*, www.rfdesign.com

Glidden, R. et al. (2004). Design of ultra-low-cost UHF RFID tags for supply chain applications, *Communications Magazine, IEEE*, vol. 42, pages 140-151

Han, Y.; Li, Q. & Min, H. (2004). System modeling and simulation of RFID, *In Auto-ID Labs Research Workshop*, Zurich, Switzerland

Hashemi, H. (1993). The Indoor Radio Propagation Channel, *Proceedings of the IEEE*, vol. 81, no. 7

IDA. (2008). Infocom Development Authority of Singapore (IDA), IDA TS SRD Technical Specification for Short Range Devices, Issue 1 Rev 3, January 2008, Singapore

ISO Standards. (2007). ISO 18000-6C Standard – RFID UHF Air Interface, *Information technology – Radio frequency identification for item management – Part 6: Parameters for air interface communications at 860 MHz to 960 MHz*

Jin, C.; Cho, S. H. & Jeon, K. Y. (2007). Performance Evaluation of RFID EPC Gen2 Anti-collision Algorithm in AWGN Environment, *International Conference on Mechatronics and Automation*, 5-8 Aug 2007, pages 2066-2070

Kajiwara, A. (2000). Circular polarization diversity with passive reflectors in indoor radio channel, *IEEE Transactions on Vehicle Technology*, May 2000, vol. 49, no. 3, pages 778–782

Karthaus, U. & Fischer, M. (2003). Fully integrated passive UHF RFID transponder IC with 16.7 uW minimum RF input power, *IEEE Journal of Solid-State Circuits*, vol. 38, No. 10, October 2003, pages 1602-1608

Kim, D.; Ingram, M.A. & Smith, W.W., Jr. (2003). Measurements of small-scale fading and path loss for long-range RF Tags, *IEEE Transactions on Antennas and Propagation*, vol. 51, No. 8, August 2003, pages 1740-1749

Leong, K. S.; Ng, M. L. & Cole, P. H. (2006). Positioning Analysis of Multiple Antennas in a Dense RFID Reader Environment, *International Symposium on Applications and the Internet Workshop 2006*, 23-27 Jan 2006, pages 56-59

Mayer, L. W.; Wrulich, M. & Caban, S. (2006). Measurements and Channel Modeling for Short Range Indoor UHF Applications, *Proceedings of The European Conference on Antennas and Propagation*, EuCAP 2006, 6-10 Nov. 2006, Nice, France

Mitsugi, J. & Hada, H. (2006). Experimental Study on UHF passive RFID Readability Degradation, *SAINT Workshops 2006*, pages 52-55

Mitsugi, J. & Shibao, Y. (2007). Multipath Identification using Steepest Gradient Method for Dynamic Inventory in UHF RFID, *International Symposium on Applications and the Internet Workshops 2007 (SAINT Workshops 2007)*

Mitsugi, J. & Tokumasu, O. (2008). A Practical Method for UHF RFID Interrogation Area Measurement Using Battery Assisted Passive Tag, *IEICE Transactions on Communications*, vol. E91-B, No.4, pages 1047-1054

Muehlmann, U. & Witschnig, H. (2007). Hard to read tags: an application-specific experimental study in passive UHF RFID systems, *elektrotechnik und informationstechnik*, vol. 11, pp. 391-396, Vienna, Austria: Springer

Nikookar, H. & Hashemi, H. (1993). Statistical Modeling of Signal Amplitude Fading Of Indoor Radio Propagation Channels, *Proc. of Int. Conf. on Universal Personal Communications*, vol. 1, pages 84-88

Ramakrishnan, K. & Deavours, D. (2006). Performance benchmarks for passive UHF RFID tags, *Proceedings of the 13th GI/ITG Conference on Measurement, Modeling, and Evaluation of Computer and Communication Systems*, pages 137-154

Rappaport, T. S. (2002). *Wireless Communications – Principles and Practice*, Prentice Hall, Second Edition

Rappaport, T.S. & McGillem, C.D. (1989). UHF fading in factories, *IEEE Journal Selected Areas of Communications*, Vol. 7, No. 1, January 1989, pages 40-48

Redemske, R. & Fletcher, R. (2005). The Design of UHF Tag Emulators with Applications to RFID testing and Data Transport, *Proceedings of 4th IEEE Conference on Automatic Identification Technologies*, October 2005

Ross, R.A. (1966). Radar cross section of rectangular flat plates as a function of aspect angle, *IEEE Transactions on Antennas and Propagation*, July 1966, vol. 14, no. 3, pages 329–335

Sato, K.; Manabe, T., Polivka, J., Ihara, T., Kasashima, Y. & Yamaki, K. (1996). Measurement of the Complex Refractive Index of Concrete at 57.5 GHz, *IEEE Transactions on Antennas and Propagation*, vol. 44, no. 1, pages 35-40.

Saunders, S. R. (1999). *Antennas and Propagation for Wireless Communication Systems*, ISBN: 978-0-471-98609-6, 426 pages, 10/1999

SRRC. (2007). State Radio Regulation Committee (SRRC), Ministry of Informatics Industry (MII), P.R.China, 800/900 MHz Radio Frequency Identification (RFID)

Vogt, H. (2002). Multiple object identification with passive RFID tags, *IEEE International Conference on Systems, Man and Cybernetics*, vol: 3, 6-9 Oct. 2002

Wang, L. C. & Liu, H. C. (2006). A Novel Anti-Collision Algorithm for EPC Gen2 RFID Systems, Wireless *Communication Systems, 2006. ISWCS '06*, Sept. 2006, pages 761-765

Development and Implementation of RFID Technology

Edited by Cristina Turcu

ISBN 978-3-902613-54-7
Hard cover, 450 pages
Publisher I-Tech Education and Publishing
Published online 01, January, 2009
Published in print edition January, 2009

The book generously covers a wide range of aspects and issues related to RFID systems, namely the design of RFID antennas, RFID readers and the variety of tags (e.g. UHF tags for sensing applications, surface acoustic wave RFID tags, smart RFID tags), complex RFID systems, security and privacy issues in RFID applications, as well as the selection of encryption algorithms. The book offers new insights, solutions and ideas for the design of efficient RFID architectures and applications. While not pretending to be comprehensive, its wide coverage may be appropriate not only for RFID novices but also for experienced technical professionals and RFID aficionados.

INTECH
open science | open minds

InTech Europe
University Campus STeP Ri
Slavka Krautzeka 83/A
51000 Rijeka, Croatia
Phone: +385 (51) 770 447
Fax: +385 (51) 686 166
www.intechopen.com

InTech China
Unit 405, Office Block, Hotel Equatorial Shanghai
No.65, Yan An Road (West), Shanghai, 200040, China
中国上海市延安西路65号上海国际贵都大饭店办公楼405单元
Phone: +86-21-62489820
Fax: +86-21-62489821